Dramatic consequences of reducing erythrocyte membrane cholesterol on *Plasmodium falciparum*

Avantika I. Ahiya[a], Suyash Bhatnagar[a], Joanne Morrisey[a], Josh R. Beck[b], Akhil B. Vaidya[a*]

a. *Center for Molecular Parasitology, Institute for Molecular Medicine and Infectious Disease, Department of Microbiology and Immunology, Drexel University College of Medicine, Philadelphia, Pennsylvania 19129*

b. *Department of Biomedical Sciences, Iowa State University, Ames, Iowa 50011*

*To whom correspondence should be addressed at Center for Molecular Parasitology, Dept. of Microbiology and Immunology, Drexel University College of Medicine, 2900 Queen Lane, Philadelphia, PA 19129. Tel.: 215-991- 8557; Fax: 215-848-2271;

E-mail: av27@drexel.edu

Abstract

During its blood stage development, the malaria parasite establishes an active cholesterol gradient across the various membrane systems within the infected erythrocyte. We have observed certain antimalarial compounds to disrupt cholesterol homeostasis in intraerythrocytic stages of *Plasmodium falciparum*. Previously, reduction of cholesterol from the erythrocyte membrane by treatment with methyl-ß-cyclodextrin (MßCD) was shown to inhibit parasite invasion and growth. In addition, MßCD treatment of trophozoite stage *P. falciparum* was shown to result in parasite expulsion from the host cell. We have revisited these phenomena by using live video microscopy, ultrastructural analysis, and response to antimalarial compounds. By using time-lapse video microscopy of fluorescently tagged parasites, we show that MßCD treatment for just 30 min causes dramatic expulsion of the trophozoite stage parasites. This forceful expulsion occurs within 10 sec. Remarkably, the plasma membrane of the host cell from which the parasite has been expelled does not appear to be compromised. The parasitophorous vacuolar membrane (PVM) continued to surround the extruded parasite, but the PVM appeared damaged. Treatment with antimalarial compounds targeting PfATP4 or PfNCR1 prevented MßCD-mediated extrusion of the parasites, pointing to a potential role of cholesterol dynamics underlying the expulsion phenomena. We also confirmed the essential role of erythrocyte plasma membrane cholesterol for invasion and growth of *P. falciparum*. This defect can be partially complemented by cholesterol and desmosterol but not with epicholesterol, revealing stereospecificity underlying cholesterol function. Overall, our studies advance previous observations and reveal unusual cell biological features underlying cholesterol depletion of infected erythrocyte plasma membrane.

Keywords:

Malaria, *Plasmodium falciparum*, parasite extrusion, cholesterol dynamics, PfATP4 and PfNCR1 inhibitors, vomocytosis

41 **Introduction:**

42 A salient feature of malaria parasites is their dependence on the host to fulfil their nutrient
43 requirements. In addition to various nutrients, *Plasmodium* salvages lipids and fatty acids from the
44 host. While the parasite possesses pathways for synthesizing and modifying lipids (1, 2), it lacks the
45 machinery for *de novo* cholesterol synthesis (3-6). Unlike the intrahepatic stages where the parasites
46 have access to copious amounts of cholesterol (7), blood stage parasites can only access cholesterol
47 present in the erythrocyte membrane (8). Recent studies from our laboratory have identified
48 antimalarials that inhibit two parasite plasma membrane (PPM) transporters, PfATP4 and PfNCR1,
49 which disrupt cholesterol and lipid homeostasis in the PPM (9, 10). Upon treatment with these
50 compounds, there is a rapid accumulation of cholesterol in the PPM rendering the parasites sensitive
51 to the cholesterol dependent detergent saponin. This was observed as the loss of cytosolic proteins in
52 drug treated parasites exposed to saponin. This effect was reversible indicating an active mechanism
53 of cholesterol dynamics within the parasite (9). These unexpected consequences of exposure to novel
54 antimalarials suggest the presence of mechanisms that influence cholesterol transport within
55 intraerythrocytic *P. falciparum*. Previously, it was shown that intra-erythrocytic *P. falciparum* growth
56 requires a supply of fatty acids that cannot be substituted with lipids and cholesterol from serum
57 derived lipoproteins (11). Furthermore, studies from the Haldar laboratory have shown that
58 cholesterol in the erythrocyte plasma membrane is essential for invasion and growth of *P. falciparum*.
59 Interestingly, reduction of cholesterol from the erythrocyte plasma membrane by treatment with
60 MßCD resulted in extrusion of the trophozoite stage parasites (12).

61 Given the observations regarding effects of new antimalarials on cholesterol dynamics and
62 the consequences of cholesterol reduction from infected erythrocyte plasma membrane, we wished to
63 examine a potential link between these phenomena. We have used live fluorescence video
64 microscopy, transmission electron microscopy and treatment with antimalarials to revisit previous
65 findings regarding the consequences of MßCD treatment of intra erythrocytic *P. falciparum*. Results
66 from our experiments confirm and extend these observations and raise important mechanistic
67 questions regarding the role of cholesterol in *P. falciparum* biology.

68 **Results:**

69

70 ***Dramatic expulsion of trophozoite stage parasites upon treatment with*** MβCD

71 A previous study showed that treatment of trophozoite stage parasites with MβCD releases
72 the parasites from the erythrocyte. In this study, the authors used filipin and ethidium bromide
73 staining of glutaraldehyde-fixed parasites and did not assess disposition of PVM and PPM in extruded
74 parasites (13). We aimed to examine this effect in real-time using time lapse video microscopy as well
75 as to assess the disposition of PVM and PPM. For this purpose, we used two different transgenic *P.*
76 *falciparum* lines, one expressing PPM-localized PfVP1 tagged with mNeonGreen, and the other
77 expressing PVM-localized EXP2 tagged with mRuby3 as well as the RhopH complex protein
78 RhopH2 tagged with mNeonGreen. RhopH2 is initially stored in merozoite rhoptries and secreted into
79 the parasitophorous vacuole (PV) during invasion, eventually trafficking to the host cell membrane
80 (14). The use of these parasite lines permitted us to monitor the PPM, PVM and rhoptries of the
81 parasite when exposed to MßCD. The trophozoites and early schizont stage-infected erythrocytes
82 were attached to poly-L-lysine coated plates, stained with fluorescent probes for the RBC membrane
83 and nuclei followed by treatment with MßCD for 30 mins. MßCD was removed by washing with the
84 culture medium and the parasites were observed by live time-lapse fluorescent video microscopy. As
85 shown in Fig. 1A and Supplementary Video 1, the parasite extruded out of the host erythrocyte in a
86 dramatic fashion. This forceful transition from being intracellular to being extracellular occurred in
87 less than 10 seconds. The extruded parasites were enclosed within the PPM (in green, Fig. 1B) as well
88 as the PVM (in red, Fig. 1C). Depending upon the plane from which the parasite emerges from the
89 erythrocyte, parts of the PVM were observed still tethered to the host cell. The extrusion phenomenon
90 was limited to mature stage parasites. Cholesterol depletion of ring stage parasites did not result in
91 extrusion; RhopH2 was partially localized to the erythrocyte plasma membrane in the ring stage
92 parasites, but the parasite remained inside the host cell (Fig. 1D, Supplementary video 3).
93 Quantification of this phenomenon showed that about 70% of the mature stage parasites extruded
94 upon MßCD treatment (Fig. 1E).

95 The forceful expulsion of the parasite from the host cell remains mechanistically unexplained.
96 MßCD treatment of mammalian cells has been shown to affect actin polymerization (15). Thus one
97 possibility could be that rearrangement and polymerization of RBC cytoskeletal actin may underlie
98 the parasite extrusion. To test this, we treated trophozoite-infected erythrocytes with the actin
99 polymerization inhibitor, Cytochalasin D (CytD) (16). Treatment with CytD prior to MßCD treatment
100 did not inhibit MßCD mediated extrusion of the parasites. Treatment with CytD alone did not cause
101 the parasites to extrude out; however, we did observe defects in the PVM of the CytD treated parasites
102 (Fig. 1F, Supplementary video 2). Although CytD did affect the morphology of the PVM, it failed to
103 prevent extrusion of the parasites when exposed to MßCD.
104 To assess the disposition of membranes of extruded parasites in some detail, we performed
105 transmission electron microscopy of mature stage parasites treated with MßCD. The extruded
106 parasites were still surrounded by the PVM, but the PVM was compromised at multiple places (Fig.
107 1G). The PPM on the other hand remained intact with minimal changes in the intracellular structures.
108 Images shown here are representative of multiple electron micrographs.
109
110 ***Prior Treatment with novel antimalarials abrogates MßCD mediated parasite extrusion***
111 We have previously shown that inhibition of PPM transporters, PfATP4 or PfNCR1 alter
112 cholesterol dynamics in the PPM of mature stage parasites (9, 10, 17). We therefore examined the
113 effects of these cholesterol homeostasis disruptors on MßCD-mediated extrusion phenomenon. We
114 treated mature stage parasites for 2 hours with KAE609 (a PfATP4 inhibitor), MMV009108 (a
115 PfNCR1 inhibitor) or chloroquine (a heme detoxification inhibitor) followed by cholesterol depletion
116 with MßCD. Interestingly, the parasite extrusion was greatly reduced by prior exposure to PfATP4
117 and PfNCR1 inhibitors but not by chloroquine (Fig. 2A). Quantitation of this phenomenon showed
118 that 80% of parasites treated with DMSO or chloroquine extruded following MßCD treatment,
119 whereas only about 25% did so following treatment with PfATP4 and PfNCR1 inhibitors (Fig. 2B).
120 This quantitation was also supported by observation of intracellular and extracellular parasites in
121 Giemsa-stained thin blood smear (Fig. 2C and D). These results suggest that disruption of normal

122 cholesterol dynamics in mature stage parasite results in inhibition of MßCD mediated extrusion of
123 parasites.
124
125 ***Role of erythrocyte plasma membrane cholesterol in invasion and the intra-erythrocytic***
126 ***development of P. falciparum***
127 Previous studies have shown that reduction of erythrocyte plasma membrane cholesterol by
128 treatment with MßCD resulted in inhibition of parasite growth (12). Since we found that the ring stage
129 parasites were not extruded from the erythrocyte by MßCD treatment, we went on to examine the
130 effects of MßCD treatment of ring stage parasites for their intra-erythrocytic developmental cycle
131 (IDC). In addition, we also examined the consequence of complementing cholesterol depleted ring
132 stage parasites with different sterols such as cholesterol, desmosterol or epicholesterol (structures
133 shown in Fig. 3A). We treated the ring stage infected erythrocytes with MßCD for 30 mins followed
134 by washes with normal culture medium. Development of ring stage parasites was assessed by
135 examination of Giemsa-stained thin smears. As shown in Fig. 3B, parasites in the control cells
136 proceeded normally through the IDC and formed trophozoites and rings. In contrast, ring stage
137 parasites growing in cholesterol depleted erythrocytes (MßCD treated) progressed to form what
138 appeared to be trophozoites but failed to mature. Reconstitution with MßCD saturated with
139 cholesterol (CD/Cho) or desmosterol (CD/Des) appeared to restore normal IDC progression. On the
140 other hand, reconstitution with epicholesterol (CD/Epi) did not restore normal IDC, suggesting the
141 importance of stereospecificity of cholesterol polar moiety in supporting parasite development. We
142 also attempted to reconstitute with lanosterol or ß-sitosterol but could not assess it since these resulted
143 in lysis of erythrocytes. To assess the viability of the ring stage parasites growing in MßCD-treated or
144 sterol-reconstituted erythrocytes, we split the culture 1:10 into untreated normal erythrocytes. This
145 was followed by measuring parasitemia over a subsequent four-day period. As shown in Fig 3C, ring
146 stage parasites growing in cholesterol-depleted or epicholesterol-reconstituted cells failed to
147 propagate over the next two cycles. On the other hand, cholesterol- or desmosterol-reconstituted ring
148 stage parasites were able to propagate at a level of about 50% compared to the control ring stage
149 parasites. To assess progression of ring stage parasites, we measured hypoxanthine incorporation

150 over a 24-hour period. As shown in Fig 3D, there was significant reduction in hypoxanthine
151 incorporation in MßCD treated and epicholesterol reconstituted parasites, whereas ring stage parasites
152 in cholesterol or desmosterol reconstituted cells were able to incorporate hypoxanthine.
153 We examined the parasites by transmission electron microscopy at 24 and 48 hours in control
154 and following MßCD treatment. As expected at 24 hours the trophozoites in the control group
155 displayed normal morphology with distinctive internal structures and normal hemozoin formation and
156 went on to form ring stages at 48 hours (Fig 3E, top panel; Supplementary Fig. 1). In contrast MßCD
157 treated ring stages showed abnormal morphology with diminished food vacuoles at 24 hours. These
158 parasites failed to develop into normal schizonts and did not egress at 48 hours after MßCD treatment.
159 (Fig 3E, lower panel; Supplementary Fig 1). These results suggest a defect in normal trophozoite
160 development in erythrocytes with depleted cholesterol content.
161 We also assessed the ability of merozoites to invade and establish infection in MßCD treated
162 erythrocytes. MßCD treated erythrocytes were added to Percoll enriched schizonts. As shown in Fig
163 4A, reduced cholesterol content in uninfected erythrocytes prevented merozoite invasion. The
164 merozoites appeared to remain attached to the surface of MßCD treated erythrocytes but failed to
165 penetrate. Importantly, reconstitution of MßCD treated RBCs with cholesterol complemented this
166 invasion defect (Fig. 4B). Furthermore, the parasites were able to grow in these reconstituted
167 erythrocytes and undergo normal IDC progression. Splitting the cultures 1:10 with addition of normal
168 erythrocytes resulted in continued normal IDC progression of parasites from control and cholesterol
169 reconstituted cells but not from cholesterol deficient cells (Fig. 4C).
170 Different *P. falciparum* strains invade using different pathways: a sialic acid dependent or a
171 sialic acid independent pathway (18, 19). To see if cholesterol in the erythrocyte membrane is
172 selective for a given pathway, we added schizonts of either NF54 (sialic acid dependent) or Dd2
173 (sialic acid independent) strains to MßCD treated erythrocytes. Merozoites from neither strain were
174 able to invade MßCD treated erythrocytes (Fig. 4D).
175
176
177

178 **Discussion**:

179 Using live video microscopy of fluorescently tagged parasites, we have extended previous
180 observations showing expulsion of trophozoite stage *P. falciparum* upon treatment with MßCD. We
181 also showed that this expulsion is inhibited by new antimalarial compounds that disrupt cholesterol
182 homeostasis in the parasite. The dramatic expulsion of the trophozoite stage parasites following
183 MßCD treatment remains unexplained. It is hard to perceive how an intracellular parasite can escape
184 out of the host erythrocyte without causing the lysis of the host membrane in response to reduction in
185 the cholesterol content in the erythrocyte plasma membrane. The force with which the expulsion
186 appears to occur suggest an active process mediated either by the host or the parasite. Our observation
187 that Cytochalasin D did not prevent expulsion of trophozoites indicates that actin polymerization is
188 not required for this process. Osmotic pressure build-up through solute uptake in trophozoites
189 resulting in their release from the host cells has been widely used for synchronization of blood stage
190 *P. falciparum*. However, this requires incubation with high concentrations of solutes such as sorbitol.
191 At 5 mM concentration, MßCD exposure does not pose an osmotic challenge, and at ~1300 Da
192 molecular weight MßCD would not be taken up by the trophozoite-infected erythrocyte through its
193 new permeability pathway. These observations suggest the possibility of a hitherto unrecognized
194 process through which the parasite might sense cholesterol content of the erythrocyte membrane.
195 MßCD-mediated expulsion of the parasite resembles expulsion of fungal pathogens from the
196 mammalian cells through a process termed vomocytosis wherein the expulsion does not result in lysis
197 of the host cell (20-22). However, vomocytosis occurs over a period of hours whereas the expulsion
198 of the trophozoite happens in seconds, suggesting that these two phenomena occur though distinct
199 mechanistic processes.

200 Inhibition of the parasite expulsion by compounds that inhibit PfATP4 or PfNCR1was
201 unexpected; this inhibition was not a result of parasite demise since chloroquine failed to do so. Since
202 we have previously shown that these inhibitors induce cholesterol accumulation in the PPM in a
203 reversible manner, we can envision dynamic movement of cholesterol between various membranes of
204 infected erythrocytes. Recent investigations have also supported the notion of cholesterol gradients in

205 infected erythrocytes (23-27). Reduction of the plasma membrane cholesterol content, thus, appears to
206 be sensed by the parasite in a manner that results in the expulsion of trophozoites.
207 The erythrocyte plasma membrane contains large amounts of cholesterol (50 mole% of total
208 lipids). Upon infection by *Plasmodium*, the PVM acquires cholesterol but the PPM remains highly
209 deficient in cholesterol. Indeed, this fact is the basis for widely used saponin mediated freeing of
210 intra-erythrocytic parasites. Previous studies have suggested the importance of cholesterol for *P.*
211 *falciparum* growth and invasion (12, 13, 24). A recent study using lattice light scattering microscopy
212 demonstrated the importance erythrocyte membrane remodeling for the formation of the PVM, a
213 process in which cholesterol is likely to play a significant role [11]. We observed that that ring stage
214 parasites growing in cholesterol deficient erythrocytes fail to fully progress. Furthermore, the
215 digestive vacuoles of trophozoite-like parasites at 24 hours after MßCD treatment of ring stages had
216 unusual morphology (Fig.3E and Supplementary figure 1). At 48 hours after MßCD treatment of ring
217 stages, parasites appeared to attempt segmentation without being able to form mature merozoites (Fig.
218 3E and Supplementary figure 1). One possible explanation could be that cholesterol dynamics assist
219 lipid and/or fatty acid import to sustain parasite growth. The fact that cholesterol and desmosterol (but
220 not epicholesterol) could substantially rescue these defects suggest stereospecificity in the role of
221 cholesterol to sustain parasite growth. Further studies will be required to gain mechanistic insights
222 into cholesterol dynamics and their contribution to parasite growth.
223
224
225 **Methods**:
226 **Parasite lines and culture conditions**

227 Experiments were carried out using different *P. falciparum* tagged lines. 1) the 3D7 strain in
228 which endogenous PfVP1 gene was tagged with mNeon green (mNG) at the C-terminal end
229 (PfVP1-mNG) (28). This line was used for monitoring the dynamics of the parasite plasma
230 membrane; 2) the NF54 strain in which endogenous RhopH2 gene was tagged with mNG and

231 the endogenous Exp2 gene tagged with mRuby3 (NF54 Rhoph2/Exp2). Cloning was carried
232 out with Infusion (Clontech) and NEBuilder HiFi (NEB). To generate an endogenous EXP2-
233 mRuby3 fusion, 5' and 3' homology flanks targeting the 3' end of *exp2* were PCR amplified
234 from plasmid pyPM2GT-EXP2-mNG (29) using primers
235 CACTATAGAACTCGAGGGAGAAACAATCTTTTATATAAAATGTACAGAGTTTGA
236 AAG and
237 TCCTCCACTTCCCCTAGGTTCTTTATTTTCATCTTTTTTTTCATTTTTAAATAAATC
238 TCCAC and inserted between *XhoI* and *AvrII* sites in the plasmid pbPM2GT (30). The
239 mRuby3 coding sequence was then amplified from plasmid pLN-HSP101-SP-mRuby3(31)
240 using primers GATGAAAATAAAGAACCTAGGGGAAGTGGAGGAGTG and
241 TAACTCGACGCGGCCGTCACTTGTACAGCTCGTCCATGCC and inserted between
242 *XhoI* and *AvrII*, resulting in the plasmid pbEXP2-mRuby3. This plasmid was linearized at the
243 *AflII* site between the 3′ and 5′ homology flanks and co-transfected with pUF-Cas9-EXP2-
244 CT-gRNA into NF54^{attB}::HSP101^{DDD} (31) . Parasites were maintained in 10 µM trimethoprim
245 (TMP) to stabilize the HSP101^{DDD} fusion and selection with 2.5 µg/ml Blasticidin S was
246 applied 24 hours post transfection. A clonal line bearing the EXP2-mRuby3 fusion was
247 derived by limiting dilution after parasite returned from selection and designated
248 NF54^{attB}::HSP101^{DDD}+EXP2-mRuby3.

249 For generation of an endogenous RhopH2-mNG fusion, a gRNA target site was chosen
250 upstream of the *rhoph2* stop codon (TCTTCACTGATTTCTTTGTA) and the gRNA seed
251 sequence was synthesized as a sense and anti-sense primer pair (sense shown)
252 TAAGTATATAATATTTCTTCACTGATTTCTTTGTAGTTTTAGAGCTAGAA, annealed
253 and inserted into the *AflII* site of the plasmid pAIO3 (32), resulting in the plasmid pAIO3-
254 RhopH2-CT-gRNA. To integrate mNG at the 3' end of *rhoph2*, a 5' homology flank (up to
255 but not including the stop codon) was amplified from NF54^{attB} genomic DNA using primers

256 AATTTCATCATTATGAAAGTTCTCAGCTTAAGAAGCATATATTAAGAATATAGTT
257 TCAGA and
258 CCTCCACTTCCCCTAGGACTGCTCTTCAGAATATACAGGTTTTTTATAAGATCCTC
259 CGATATCTCCTTATATGGATCAGATATATCTGAGAAA, incorporating several
260 synonymous mutations in the seed sequence of the gRNA target site within the *rhoph2*
261 coding sequence. A 3' homology flank (beginning at the endogenous stop codon) was
262 amplified using primers
263 GTGACACTATAGAACTCGAGTAAACGTTAAAAAAAAAATATATATAAGGAGAAA
264 GCACTG and
265 TCTGAAACTATATTCTTAATATATGCTTCTTAAGCTGAGAACTTTCATAATGATGA
266 AATT, assembled in a second PCR reaction using primers
267 GTGACACTATAGAACTCGAGTAAACGTTAAAAAAAAAATATATATAAGGAGAAA
268 GCACTG and
269 CCTCCACTTCCCCTAGGACTGCTCTTCAGAATATACAGGTTTTTTATAAGATCCTC
270 CGATATCTCCTTATATGGATCAGATATATCTGAGAAA and inserted between *XhoI*
271 and *AvrII* sites in pyPM2GT-EXP2-mNG (29) resulting in the plasmid pyPM2GT-RhopH2-
272 mNG. This plasmid was linearized at the *AflII* site between the 3' and 5' homology flanks
273 and co-transfected with pAIO3-RhopH2-CT-gRNA into NF54^{attB}::HSP101^{DDD}+EXP2-
274 mRuby3. Selection with 2 µM DSM-1 was applied 24 hours post transfection (along with 10
275 µM trimethoprim). After parasites returned from selection, a clonal line containing the EXP2-
276 mRuby3 and RhopH2-mNG fusions was obtained by limiting dilution and designated
277 NF54^{attB}::HSP101^{DDD}+EXP2-mRuby3+RhopH2-mNG. This line was used for monitoring the
278 parasitophorous vacuolar membrane and to mark the parasite. *P. falciparum* parasites were
279 cultured in O^{+} human blood from Interstate Blood Bank, TN in RPMI 1640 supplemented
280 with 2g/L sodium bicarbonate, 10mg/L hypoxanthine, 15mM HEPES, 50mg/L gentamycin

281 sulphate, 0.5% AlbuMax II. Parasite culture was maintained at 2.5% hematocrit at 37 °C in
282 90% N_2, 5% CO_2, 5% O_2.

283

284 **Preparation of MßCD and MßCD-sterol complexes**

285 Parasites were treated with 5mM MßCD diluted in appropriate medium from a stock solution
286 of 25mM MßCD (Catalog no. AC377110250) in PBS in appropriate medium. Sterols
287 [Cholesterol (Sigma, C3045-25G) , Desmosterol (Steraloids, catalog no. C3150-000),
288 Epicholesterol (Steraloids, catalog no. C6730-000)] were loaded onto MßCD according to
289 previously published protocol (33). Briefly, 10 µL of 15mg/ml sterols dissolved in ethanol
290 were added to 500 µL 5% w/v MßCD, heated for 10 mins at 80°C and mixed by inverting
291 several times until the solution was clear. The above step was repeated 4 times to add a total
292 of 50µL sterol stock solution. The solution was heated until the sterols were stably
293 incorporated in MßCD (clear solution). MßCD/sterol complexes were snap frozen in dry ice
294 for 2 mins. Subsequently, the MßCD/sterol complexes were lyophilized in a speed vac until
295 all liquid had evaporated and a fluffy powered remained at the bottom of the tube and stored
296 at -20°C. Immediately before use, 375µl of medium was added to the MßCD/sterol
297 complexes and vortexed until dissolved. The MßCD/sterol complexes were sterilized using
298 0.22µm syringe filter.

299

300 **Treatment of parasitized erythrocytes with MBCD and reconstitution with**
301 **MBCD/sterol complexes**

302 Parasite cultures were synchronized by treatment with 0.5M alanine for 10 minutes.
303 Erythrocyte infected with ring stage parasites were treated with 5mM MßCD for 30 mins at
304 37C and washed 3 times with pre-warmed RPMI1640 media. Hematocrit was maintained at
305 2.5% throughout the culture and washing steps. The parasites were returned to normal culture

306 conditions. In experiments involving reconstitution with MßCD/sterol complexes, parasites
307 were first treated with MßCD as described above. Following this, the cells were incubated
308 with 1:7 dilution of MßCD/sterol complexes for 30 mins. Parasites were washed 3 times and
309 returned to normal culture conditions. Giemsa-stained thin blood smears were prepared 24
310 and 48 hours after the treatment with MßCD or after reconstitution with MßCD/sterol
311 complexes. The culture at 48 hours was split 1:10 in normal erythrocytes. Growth of the
312 parasites in these cultures were followed for 4 days by examining Giemsa stained thin blood
313 smears
314
315 **Hypoxanthine incorporation of ring stage erythrocyte treated with MßCD or**
316 **MßCD/sterol complexes**
317 Ring stage erythrocyte (1.5% parasitemia) were treated with MßCD for 30 mins and washed
318 3 times with normal medium. The hematocrit was maintained at 2.5%. MßCD-treated ring
319 stage erythrocytes were then treated with either MßCD/cholesterol, MßCD/desmosterol or
320 MßCD/epicholesterol for 30 mins and washed 3 times with low hypoxanthine medium. The
321 hematocrit was then adjusted to 1.5% by addition of low hypoxanthine medium to the cells.
322 200µl of cells were then plated in triplicates in a 96-well plate. Each well was pulsed with 22
323 µl of 0.5 µCi/ml ^{3}H-hypoxanthine (PerkinElmer NET 177) and incubated for 24 hours at
324 37ºC in 5% CO_2, 5% O_2, 90% N_2 chamber. Parasites were lysed by freeze/thaw and were
325 collected on filters using a cell harvester (PerkinElmer LifeSciences). This was followed by
326 addition of MicroScint O scintillation cocktail and incorporation of ^{3}H-hypoxanthine was
327 measured using a TopCount scintillation counter (PerkinElmer Life-sciences).
328
329 **Parasite invasion in MßCD or MßCD/Cholesterol treated erythrocytes**

330 We treated 500 µl of 50% hematocrit erythrocytes with 5mM MßCD for 30 mins followed by
331 3 washes. In addition, similarly treated erythrocytes were reconstituted with
332 MßCD/Cholesterol for 30 mins followed by 3 washes. Synchronized late stages trophozoites
333 were enriched by centrifugation over a 70% Percoll cushion (3000 RPM, 20 mins) and
334 washed thrice with medium. Enriched late stage trophozoites were added to MßCD-treated,
335 MßCD/Cholesterol-reconstituted and control erythrocytes. Giemsa-stained thin blood smears
336 were prepared 24 and 48 hours following the addition. The culture at 48 hours was split 1:10
337 in normal erythrocytes. Growth of the parasites in these cultures were followed for 4 days by
338 examining Giemsa-stained thin blood smears.
339
340
341 **Live microscopy of parasites**
342 Glass bottom culture dishes (35 mm) were coated with 0.1% poly-L-lysine overnight and
343 washed 3 times with PBS. Parasite culture (250µl at 2.5% hematocrit) was added to the
344 dishes and incubated for 30 mins to allow attachment. Culture dishes were washed 3 times
345 with PBS followed by addition of medium. For MßCD extrusion experiments with NF54
346 Rhoph2/Exp2 line, all washes, incubation and imaging was done in medium supplemented
347 with TMP. Parasites were attached to poly-L-lysine coated plates and incubated in RPMI
348 containing wheat germ agglutinin-Alexa 350 (WGA-350) (Invitrogen, Catalog no. W7024) at
349 5µg/ml final concentration and incubated for 12 mins to stain the erythrocyte plasma
350 membrane. In addition to WGA staining, PfVP1-mNG line was also stained with SYTO deep
351 red nuclear stain for 30 min. Parasites were treated with 5mM MßCD followed by three
352 washes with medium. The medium was replaced with phenol red free medium followed by
353 live fluorescent microscopy. Imaging was done using the Nikon Ti microscope. WGA-Alexa-
354 350 was visualized using DAPI filter set, mNeon green with FITC, SYTO deep red nuclear

355 stain with Cy5 and mRuby was visualized using TRITC filter set. Video microscopy
356 parameters are given in the legends of Supplementary Videos.
357
358 **Inhibition of MßCD mediated extrusion by novel antimalarials**.
359 To look at the effects of antimalarials on MßCD mediated extrusion, parasites were stained
360 with WGA-350 and SYTO deep red for PfVP-1mNG line or WGA-350 for NF54
361 Rhoph2/Exp2 line as described above and treated with 10xEC_{50} concentrations of
362 Choloroquine (150nM), KAE609 (10nM) or MMV009108(1μM) for 2.5 hours prior to 30
363 mins treatment with MßCD and washed thrice with medium. Medium supplemented with
364 drugs (at the concentration mentioned above) was added back to the dish and live fluorescent
365 imaging was carried out. Quantification of parasites remaining inside/outside of erythrocytes
366 was carried out by examining at least 100 different images of individual parasites for each
367 experimental condition.
368 **Cytochalasin D (Cyt-D) treatment prior to MßCD treatment of parasites**
369 Attached NF54 RhopH2/Exp2 trophozoites were stained with WGA-350 for 12 mins,
370 followed by three washes. The cells were then treated with 0.5μM Cyt-D for 45 mins. This
371 was followed by the addition of 5mM MßCD for 30 mins. The culture dishes were washed 3
372 times and live fluorescent microscopy was performed to examine parasite extrusion. In the
373 control condition, parasites were treated with Cyt-D without MßCD treatment.
374
375 **Transmission electron microscopy of trophozoite infected MßCD treated erythrocytes**
376 Erythrocytes infected with trophozoite stage parasites were treated with 5mM MBCD for 30
377 mins at 2.5% hematocrit followed by three washes with PBS and incubated in complete
378 medium for 30 mins at 37 °C. Cells were washed once in PBS by gentle centrifugation and
379 fixed with 2% paraformaldehyde, 2.5% glutaraldehyde in 100 mM cacodylate buffer and

380 were fixed for 1 hour at room temperature. Cells were gently pelleted by centrifugation,
381 resuspended in cacodylate buffer and immediately stored on dry ice for shipment.
382 Ring stage infected erythrocytes were treated with 5mM MßCD for 30 mins, washed thrice
383 with PBS and returned to culture at 37 °C. At 24 and 48 hours after the treatment, infected
384 erythrocytes were fixed and prepared for transmission electron microscopy as described
385 above.
386
387
388

389 **Acknowledgements:**
390 We thank the members of the Vaidya lab for lively discussion and input. We thank Dr.
391 Hangjun Ke for providing PfVP1-mNG parasite line. This work was supported by a National
392 Institutes of Health grant R01 AI132508 to ABV and R00 HL133453 to J.R.B.

393 **References:**

394 1. Cassera MB, Gozzo FC, D'Alexandri FL, Merino EF, del Portillo HA, Peres VJ,
395 Almeida IC, Eberlin MN, Wunderlich G, Wiesner J, Jomaa H, Kimura EA, Katzin
396 AM. 2004. The methylerythritol phosphate pathway is functionally active in all
397 intraerythrocytic stages of Plasmodium falciparum. J Biol Chem 279:51749-59.
398 2. Gerold P, Schwarz RT. 2001. Biosynthesis of glycosphingolipids de-novo by the
399 human malaria parasite Plasmodium falciparum. Mol Biochem Parasitol 112:29-37.
400 3. Holz GG, Jr. 1977. Lipids and the malarial parasite. Bull World Health Organ 55:237-
401 48.
402 4. Maguire PA, Sherman IW. 1990. Phospholipid composition, cholesterol content and
403 cholesterol exchange in Plasmodium falciparum-infected red cells. Mol Biochem
404 Parasitol 38:105-12.
405 5. Vial HJ, Ancelin ML, Philippot JR, Thuet MJ. 1990. Biosynthesis and dynamics of
406 lipids in Plasmodium-infected mature mammalian erythrocytes. Blood Cells 16:531-
407 55; discussion 556-61.
408 6. Vial HJ, Philippot JR, Wallach DF. 1984. A reevaluation of the status of cholesterol
409 in erythrocytes infected by Plasmodium knowlesi and P. falciparum. Mol Biochem
410 Parasitol 13:53-65.
411 7. Labaied M, Jayabalasingham B, Bano N, Cha SJ, Sandoval J, Guan G, Coppens I.
412 2011. Plasmodium salvages cholesterol internalized by LDL and synthesized de novo
413 in the liver. Cell Microbiol 13:569-86.

414 8. Grellier P, Rigomier D, Clavey V, Fruchart JC, Schrevel J. 1991. Lipid traffic
415 between high density lipoproteins and Plasmodium falciparum-infected red blood
416 cells. J Cell Biol 112:267-77.
417 9. Das S, Bhatanagar S, Morrisey JM, Daly TM, Burns JM, Jr., Coppens I, Vaidya AB.
418 2016. Na+ Influx Induced by New Antimalarials Causes Rapid Alterations in the
419 Cholesterol Content and Morphology of Plasmodium falciparum. PLoS Pathog
420 12:e1005647.
421 10. Istvan ES, Das S, Bhatnagar S, Beck JR, Owen E, Llinas M, Ganesan SM, Niles JC,
422 Winzeler E, Vaidya AB, Goldberg DE. 2019. Plasmodium Niemann-Pick type C1-
423 related protein is a druggable target required for parasite membrane homeostasis.
424 Elife 8.
425 11. Coppens I, Vielemeyer O. 2005. Insights into unique physiological features of neutral
426 lipids in Apicomplexa: from storage to potential mediation in parasite metabolic
427 activities. Int J Parasitol 35:597-615.
428 12. Samuel BU, Mohandas N, Harrison T, McManus H, Rosse W, Reid M, Haldar K.
429 2001. The role of cholesterol and glycosylphosphatidylinositol-anchored proteins of
430 erythrocyte rafts in regulating raft protein content and malarial infection. J Biol Chem
431 276:29319-29.
432 13. Lauer S, VanWye J, Harrison T, McManus H, Samuel BU, Hiller NL, Mohandas N,
433 Haldar K. 2000. Vacuolar uptake of host components, and a role for cholesterol and
434 sphingomyelin in malarial infection. The EMBO journal 19:3556-3564.
435 14. Ahmad M, Manzella-Lapeira J, Saggu G, Ito D, Brzostowski JA, Desai SA. 2020.
436 Live-Cell FRET Reveals that Malaria Nutrient Channel Proteins CLAG3 and RhopH2
437 Remain Associated throughout Their Tortuous Trafficking. mBio 11.
438 15. Guerra FS, Sampaio LdS, Konig S, Bonamino M, Rossi MID, Costa ML, Fernandes
439 P, Mermelstein C. 2016. Membrane cholesterol depletion reduces breast tumor cell
440 migration by a mechanism that involves non-canonical Wnt signaling and IL-10
441 secretion. Translational Medicine Communications 1:3.
442 16. Casella JF, Flanagan MD, Lin S. 1981. Cytochalasin D inhibits actin polymerization
443 and induces depolymerization of actin filaments formed during platelet shape change.
444 Nature 293:302-5.
445 17. Bhatnagar S, Nicklas S, Morrisey JM, Goldberg DE, Vaidya AB. 2019. Diverse
446 Chemical Compounds Target Plasmodium falciparum Plasma Membrane Lipid
447 Homeostasis. ACS infectious diseases 5:550-558.
448 18. Camus D, Hadley TJ. 1985. A Plasmodium falciparum antigen that binds to host
449 erythrocytes and merozoites. Science 230:553-6.
450 19. Dolan SA, Miller LH, Wellems TE. 1990. Evidence for a switching mechanism in the
451 invasion of erythrocytes by Plasmodium falciparum. J Clin Invest 86:618-24.
452 20. Cruz-Acuña M, Pacifici N, Lewis JS. 2019. Vomocytosis: Too Much Booze, Base, or
453 Calcium? mBio 10.
454 21. Nicola AM, Robertson EJ, Albuquerque P, Derengowski Lda S, Casadevall A. 2011.
455 Nonlytic exocytosis of Cryptococcus neoformans from macrophages occurs in vivo
456 and is influenced by phagosomal pH. mBio 2.
457 22. Seoane PI, May RC. 2020. Vomocytosis: What we know so far. Cell Microbiol
458 22:e13145.
459 23. Fraser M, Jing W, Bröer S, Kurth F, Sander LE, Matuschewski K, Maier AG. 2021.
460 Breakdown in membrane asymmetry regulation leads to monocyte recognition of P.
461 falciparum-infected red blood cells. PLoS Pathog 17:e1009259.
462 24. Geoghegan ND, Evelyn C, Whitehead LW, Pasternak M, McDonald P, Triglia T,
463 Marapana DS, Kempe D, Thompson JK, Mlodzianoski MJ, Healer J, Biro M,

464 Cowman AF, Rogers KL. 2021. 4D analysis of malaria parasite invasion offers
465 insights into erythrocyte membrane remodeling and parasitophorous vacuole
466 formation. Nat Commun 12:3620.
467 25. Hayakawa EH, Yamaguchi K, Mori M, Nardone G. 2020. Real-time cholesterol
468 sorting in Plasmodium falciparum-erythrocytes as revealed by 3D label-free imaging.
469 Sci Rep 10:2794.
470 26. Tokumasu F, Crivat G, Ackerman H, Hwang J, Wellems TE. 2014. Inward
471 cholesterol gradient of the membrane system in P. falciparum-infected erythrocytes
472 involves a dilution effect from parasite-produced lipids. Biol Open 3:529-41.
473 27. Koch M, Cegla J, Jones B, Lu Y, Mallat Z, Blagborough AM, Angrisano F, Baum J.
474 2019. The effects of dyslipidaemia and cholesterol modulation on erythrocyte
475 susceptibility to malaria parasite infection. Malar J 18:381.
476 28. Solebo O, Ling L, Zhou J, Fu T-M, Ke H. 2021. Plasmodium
477 falciparum vacuolar pyrophosphatase 1 for ring stage development and its
478 transition to trophozoite. bioRxiv
479 doi:10.1101/2021.10.25.465524:2021.10.25.465524.
480 29. Glushakova S, Busse BL, Garten M, Beck JR, Fairhurst RM, Goldberg DE,
481 Zimmerberg J. 2017. Exploitation of a newly-identified entry pathway into the
482 malaria parasite-infected erythrocyte to inhibit parasite egress. Sci Rep 7:12250.
483 30. Beck JR, Muralidharan V, Oksman A, Goldberg DE. 2014. PTEX component
484 HSP101 mediates export of diverse malaria effectors into host erythrocytes. Nature
485 511:592-5.
486 31. Glushakova S, Beck JR, Garten M, Busse BL, Nasamu AS, Tenkova-Heuser T,
487 Heuser J, Goldberg DE, Zimmerberg J. 2018. Rounding precedes rupture and
488 breakdown of vacuolar membranes minutes before malaria parasite egress from
489 erythrocytes. Cell Microbiol 20:e12868.
490 32. Nessel T, Beck JM, Rayatpisheh S, Jami-Alahmadi Y, Wohlschlegel JA, Goldberg
491 DE, Beck JR. 2020. EXP1 is required for organisation of EXP2 in the
492 intraerythrocytic malaria parasite vacuole. Cell Microbiol 22:e13168.
493 33. Luu W, Gelissen IC, Brown AJ. 2017. Manipulating Cholesterol Status Within Cells.
494 Methods Mol Biol 1583:41-52.
495

496

497

498

499

Figures

Figure 1:

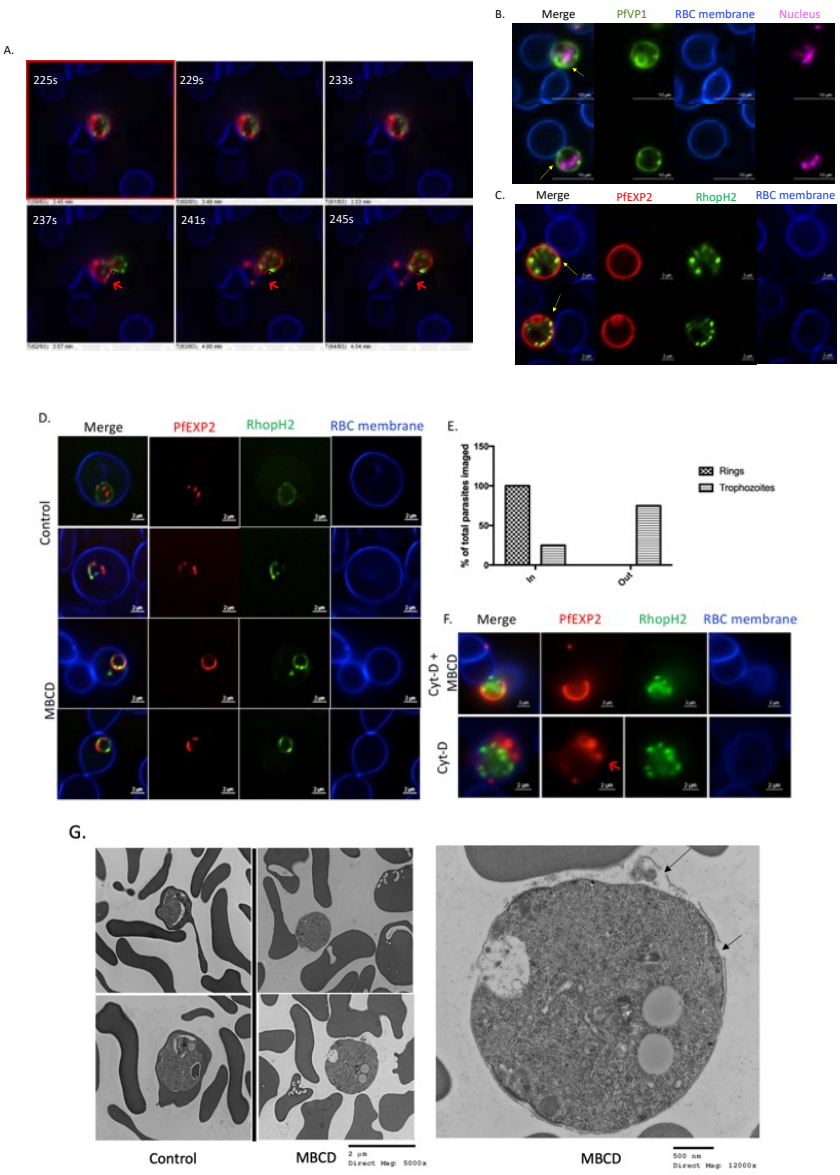

Figure 1: Trophozoites extrude out from erythrocyte upon treatment with MßCD. (A) Still frames from Supplementary video 1 from time-lapse video microscopy performed at. Parasites extrude out from the erythrocyte with the PVM still tethered to the erythrocyte membrane without causing the lysis of erythrocyte (indicated by arrows). (B) Representative images (>50) of PfVP1- mNG line after MßCD treatment. Nucleus is stained with SYTO-deep red (Pink). (C) Representative images (>50) of NF54 RhopH2/Exp2 line after MßCD

525 treatment. Erythrocyte membrane is stained with WGA-Alexa-350 (Blue). Infected
526 erythrocytes were subjected to live fluorescent microscopy after treatment with MßCD.
527 Parasites extrude out from erythrocyte without causing lysis of the erythrocyte with their PPM
528 (B) and PVM (C) still attached to the erythrocyte as indicated by the arrows. (D) Representative
529 images of erythrocytes infected with ring stages of the NF54 RhopH2/Exp2 line treated with
530 MßCD. Ring stage parasites do not extrude out from erythrocytes. (E) Quantification of
531 parasites remaining inside/outside of erythrocytes after MßCD treatment was carried out by
532 examining at least 100 different images of individual parasites for each experimental condition
533 (100 for ring stages and 330 for trophozoites). (F) Upper panel: Treatment of NF54
534 RhopH2/Exp2 trophozoites with 0.5 µM Cyt-D for 45 mins prior to MßCD treatment does not
535 inhibit parasite extrusion. Lower panel: Treatment with 0.5 µM Cyt-D alone does not cause
536 extrusion of trophozoites but did alter PVM morphology (as indicated by arrows). (G)
537 (Left)Treatment with MßCD causes extrusion of *P. falciparum* stage trophozoites without
538 causing erythrocyte rupture unlike the control group where the trophozoite is still inside the
539 erythrocyte (Scale bar- 2µM, Direct magnification-5,000x). (Right) Zoomed in image of
540 parasite extruded out of erythrocyte after MßCD treatment shows the PVM ruptured at multiple
541 places indicated by black arrows. Electron microscopy of extruded *P. falciparum*. Left panels
542 show lower magnification views of control and MβCD-treated trophozoites. A higher
543 magnification view of an extruded parasite (right panel) shows that the PVM is compromised
544 at multiple places (arrows) (Scale bar-500nM, Direct magnification-12,000x).
545

Figure 2:

546

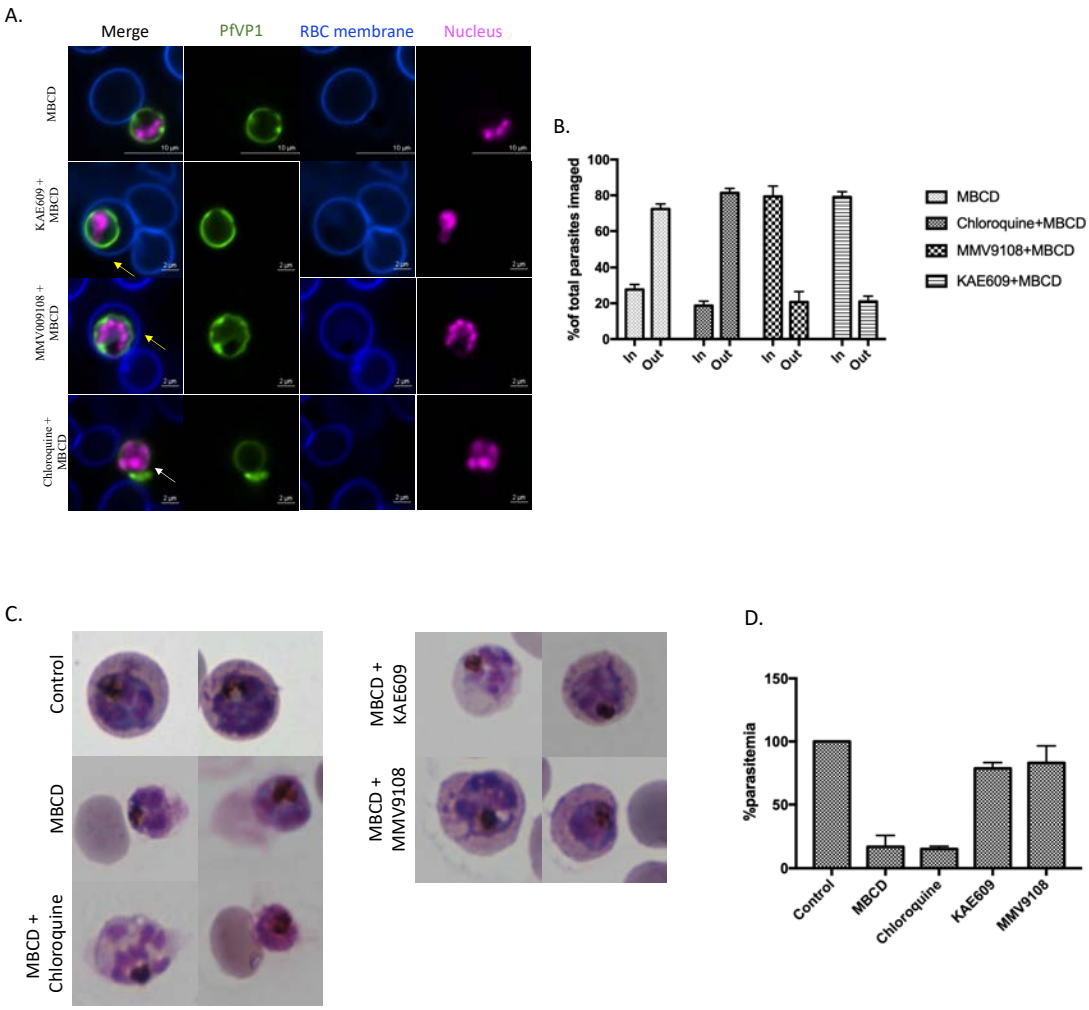

547 **Figure 2 :** Treatment with PfATP4 or PfNCR1 inhibitors prior to MßCD treatment inhibited
548 MßCD mediated extrusion of parasites: (A) Trophozoite stage parasites from PfVP1-mNG line
549 were treated with KAE609 (10nM), MMV009108 (1µM) and chloroquine (150nM) prior to
550 treatment with MßCD. Live fluorescent imaging showed that parasite extrusion was inhibited
551 by prior treatment with KAE609 and MMV009108 (indicated by yellow arrows) while
552 treatment with chloroquine like MßCD did not inhibit this extrusion (indicated by white
553 arrows). Nucleus is stained with SYTO-deep red (pink). Erythrocyte membrane is stained with
554 WGA-Alexa-350 (Blue). Representative images from 3 independent experiments for each
555 condition (B) Quantification from live fluorescent microscopy experiments of parasite
556 extrusion upon drug treatment followed by MßCD treatment. Approximately 250 cells for each
557 experimental condition over 4 independent experiment were assessed. (C) Giemsa stained thin

558 blood smears prepared from cultures after treatment with KAE609 (10nM), MMV009108
559 (1µM) and chloroquine (150nM) prior to treatment with MßCD. (D) Quantitation of parasite
560 extrusion upon drug treatment followed by MßCD treatment from Giemsa-stained thin blodd
561 smears (~1000 cells were counted).
562

Figure 3:

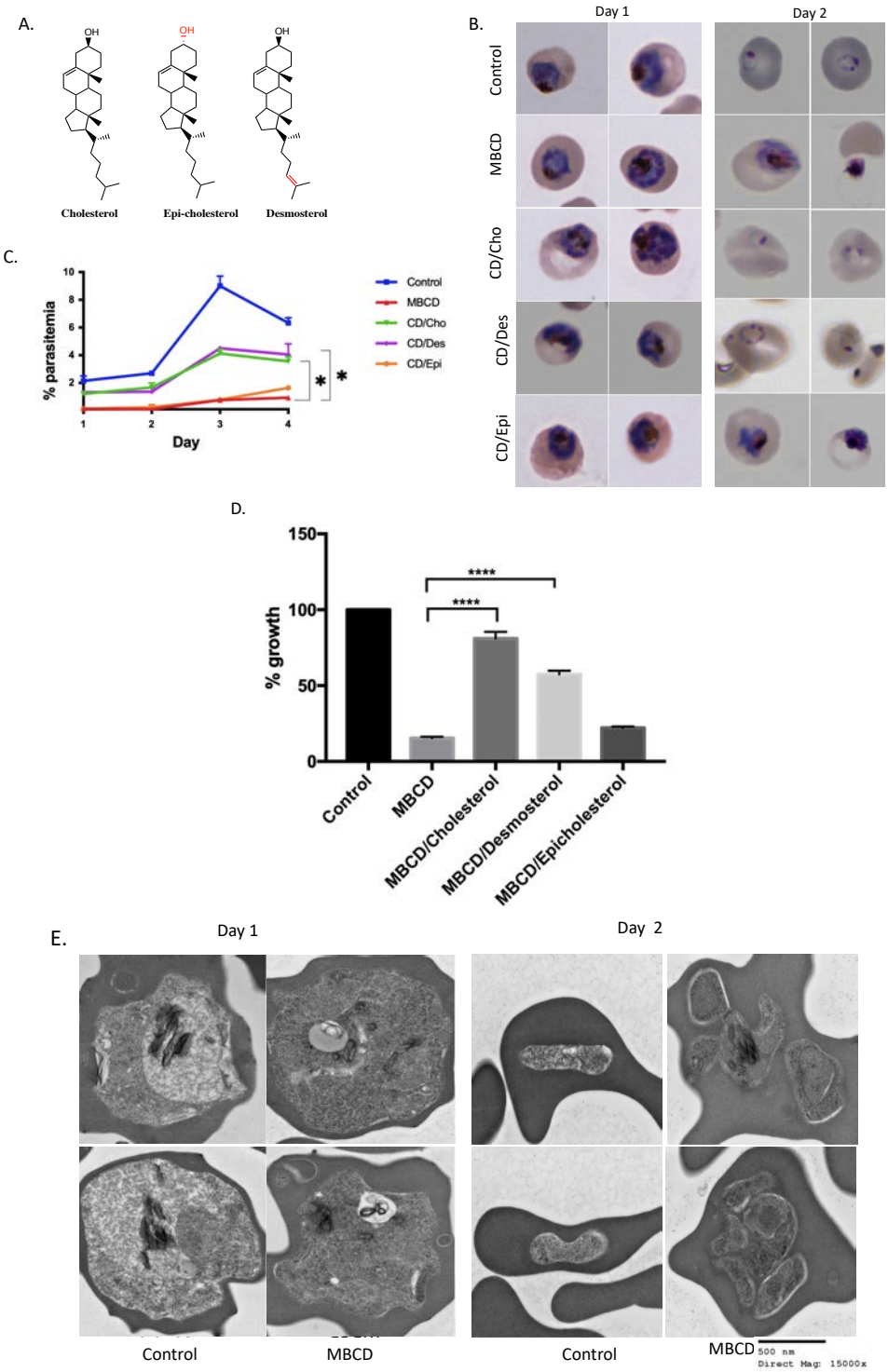

582 **Figure 3:** Cholesterol in the erythrocyte membrane is essential for growth and proliferation of
583 *P. falciparum*.
584 (A) Structure of MßCD, Cholesterol, Epicholesterol and Desmosterol. The differences between
585 the structure of sterols are highlighted in red. (B) Giemsa-stained thin blood smears prepared
586 from control, MßCD and erythrocytes reconstituted with cholesterol, desmosterol or
587 epicholesterol at 24 and 48 hours after treatment. C) Parasitemia in 1:10 split of ring stage
588 parasites from control, MßCD (CD) or erythrocytes reconstituted with cholesterol (CD/Cho),
589 desmosterol(CD/Des) or epicholesterol (CD/Epi) over 4 days (~3000 cells were counted).
590 Based on one tailed unpaired *t-test* (* $p<0.05$). (D) Relative (^{3}H)-hypoxanthine incorporation
591 by ring stage parasites over a 24 hour period following treatment with MßCD or reconstituted
592 with cholesterol, desmosterol and epicholesterol. Based on unpaired t-test with Welch's
593 correction (* $p<0.05$, *** $p<0.001$). Error bars=mean±SD N=8. (E) TEM of the ring stage
594 erythrocyte treated with 5mM MßCD and imaged after 24 or 48 hours. (Left)After 24 hours, in
595 erythrocyte treated with MßCD, parasites are unable to form normal trophozoites. The nuclear
596 membrane is indistinct, hemozoin is dispersed (indicated by arrows) and food vacuole is small
597 compared to control erythrocytes. (Right) After 48 hours, parasites in the control culture were
598 able to invade the erythrocyte and form rings while the parasites in the MßCD treated

599 erythrocytes undergo did not progress further and appear to disintegrate (Scale bar-500nM,

600 Direct magnification-15,000x).

Figure 4:

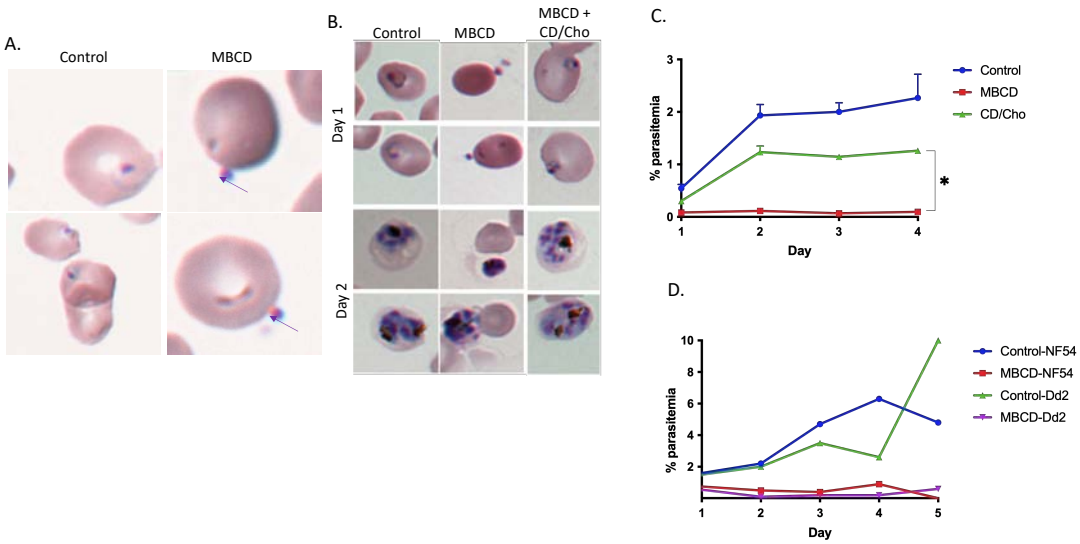

601

602 **Figure 4:** Reducing the cholesterol content in the erythrocyte membrane inhibits *P. falciparum*

603 invasion

604 (A) Giemsa stained thin blood smears from control and MßCD treated erythrocytes after 24

605 hours. While ring stages were seen in the control erythrocytes, no invasion was seen in the

606 MßCD treated erythrocytes but merozoites appeared to remain attached to the surface as

607 indicated by arrows. (B) Percoll enriched trophozoites were added to erythrocytes treated with

608 MßCD or reconstituted with cholesterol and giemsa stained thin blood smears were prepared

609 at 24 and 48 hours. Reconstituted erythrocytes were able to support parasite growth. (C)

610 Parasitemia from 1:10 spilt of culture from MßCD treated and reconstituted with cholesterol in

611 normal erythrocytes over a period of 4 days (~3000 cells were counted). Based on Mann-

612 Whitney test (* $p<0.05$) (D) Percoll synchronized trophozoites from NF54 and Dd2 strains

613 were added onto MßCD treated erythrocytes. Parasitemia from 1:10 split of these cultures by
614 examining Giemsa-stained thin blood smears (~1000 cells were counted).
615
616 **Supplementary Videos**
617 **Supplementary video 1:** Treatment with MßCD causes extrusion of trophozoites from
618 erythrocytes
619 Representative time lapse video microscopy of the NF54 RhopH2/Exp2 line after MßCD
620 treatment. Erythrocyte membrane is stained with WGA-Alexa-350 (Blue). Infected
621 erythrocytes were subjected to live fluorescent microscopy after treatment with MßCD.
622 Parasites extrude out from erythrocyte without causing lysis of the erythrocyte. Video was
623 acquired using the Nikon Ti microscope. The interval between each frame was 4 sec and the
624 video was captured for a total 20 min (93 frames, FPS:0.09, frames 59-64 shown in the
625 video). Images were deconvoluted by Richardson Lucy algorithm using the Nikon NIS
626 elements software package and converted to .avi files.
627
628 **Supplementary video 2:** Cyt-D treatment does not inhibit MßCD mediated parasite
629 extrusion
630 Representative time lapse video microscopy of the NF54 RhopH2/Exp2 line after MßCD
631 treatment. Erythrocyte membrane is stained with WGA-Alexa-350 (Blue). Infected
632 erythrocytes were subjected to live fluorescent microscopy after treatment with Cyt-D
633 followed by treatment with MßCD. Treatment with Cyt-D does not inhibit MßCD mediated
634 extrusion of the parasite. Video microscopy was performed as mentioned above for video 1.
635 The interval between each frame was 31 sec and the video was captured for a total 5 min (11
636 frames, FPS:0.04, all 11 frames shown in the video)
637

638 **Supplementary movie 3:** Treatment with MßCD does not cause extrusion of ring stage

639 parasites

640 Erythrocytes infected with ring stages of the NF54 RhopH2/Exp2 were treated with MßCD .

641 Erythrocyte membrane is stained with WGA-Alexa-350 (Blue). Ring stage parasites do not

642 extrude out after MßCD treatment. Video microscopy was performed as mentioned for video

643 1. The interval between each frame was 31 secs and the video was captured for a total 5 mins

644 (11 frames, FPS:0.04, all 11 frames shown in the video)

645

Supplementary Figure 1:

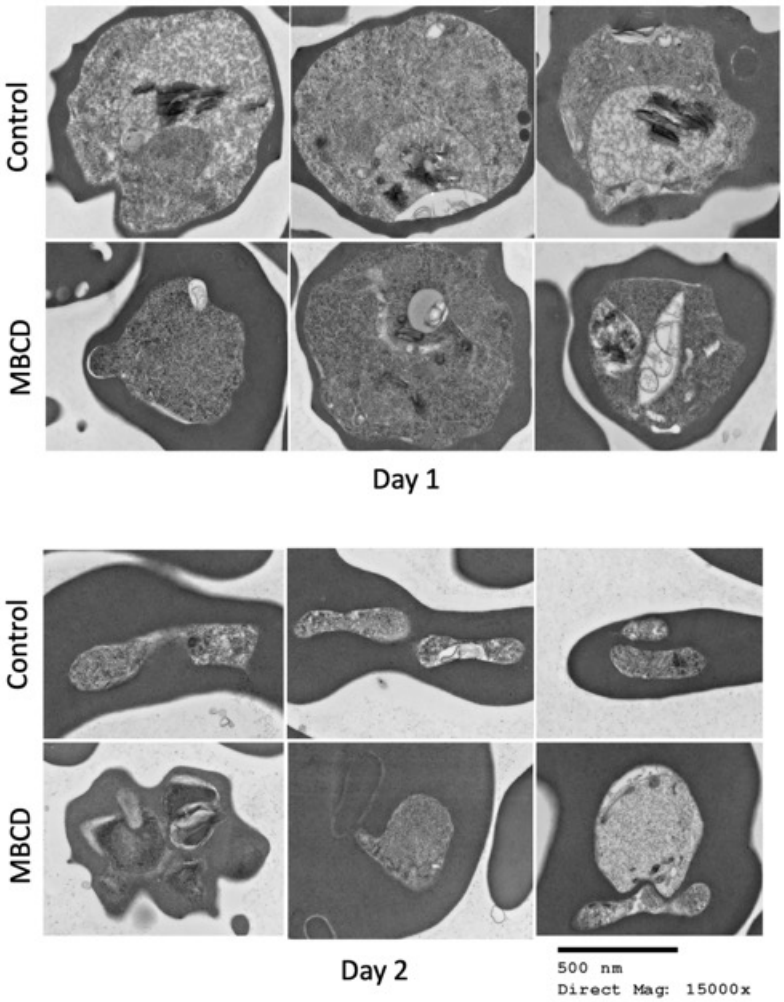

653 **Supplementary figure 1:** TEM of the ring stage erythrocyte treated with 5mM MßCD and
654 imaged after 24 (Day 1) or 48 hours (Day2)
655 (A) After 24 hours, the trophozoite like parasites in the MßCD treated cultures (lower panel)
656 have indistinct membranes, compromised food vacuole and dispersed hemozoin compared to
657 the controls (Upper panel) (B) After 48 hours, in the control culture (Upper panel) the
658 parasites invaded and formed rings while the parasites in the MßCD treated cultures (Lower
659 panel) failed to form mature merozoites (Scale bar-500nM, Direct magnification-15,000x).